

Improved measurements of the partial rate asymmetry in  $B \rightarrow hh$  decays

Y. Chao,<sup>25</sup> P. Chang,<sup>25</sup> K. Abe,<sup>7</sup> K. Abe,<sup>40</sup> H. Aihara,<sup>42</sup> Y. Asano,<sup>46</sup> T. Aushev,<sup>11</sup> S. Bahinipati,<sup>4</sup> A. M. Bakich,<sup>37</sup> Y. Ban,<sup>32</sup> I. Bedny,<sup>1</sup> U. Bitenc,<sup>12</sup> I. Bizjak,<sup>12</sup> S. Blyth,<sup>25</sup> A. Bondar,<sup>1</sup> M. Bračko,<sup>12,19</sup> J. Brodzicka,<sup>26</sup> T. E. Browder,<sup>6</sup> K.-F. Chen,<sup>25</sup> B. G. Cheon,<sup>3</sup> R. Chistov,<sup>11</sup> S.-K. Choi,<sup>5</sup> Y. Choi,<sup>36</sup> S. Cole,<sup>37</sup> M. Danilov,<sup>11</sup> M. Dash,<sup>47</sup> L. Y. Dong,<sup>9</sup> S. Eidelman,<sup>1</sup> V. Eiges,<sup>11</sup> S. Fratina,<sup>12</sup> N. Gabyshev,<sup>1</sup> T. Gershon,<sup>7</sup> G. Gokhroo,<sup>38</sup> B. Golob,<sup>12,18</sup> R. Guo,<sup>23</sup> J. Haba,<sup>7</sup> N. C. Hastings,<sup>7</sup> K. Hayasaka,<sup>21</sup> H. Hayashii,<sup>22</sup> M. Hazumi,<sup>7</sup> T. Higuchi,<sup>7</sup> L. Hinz,<sup>17</sup> T. Hokuue,<sup>21</sup> Y. Hoshi,<sup>40</sup> W.-S. Hou,<sup>25</sup> Y. B. Hsiung,<sup>25,\*</sup> T. Iijima,<sup>21</sup> A. Imoto,<sup>22</sup> K. Inami,<sup>21</sup> A. Ishikawa,<sup>7</sup> R. Itoh,<sup>7</sup> H. Iwasaki,<sup>7</sup> Y. Iwasaki,<sup>7</sup> H. Kakuno,<sup>42</sup> J. H. Kang,<sup>48</sup> J. S. Kang,<sup>14</sup> N. Katayama,<sup>7</sup> H. Kawai,<sup>2</sup> T. Kawasaki,<sup>28</sup> H. R. Khan,<sup>43</sup> H. J. Kim,<sup>16</sup> J. H. Kim,<sup>36</sup> K. Kinoshita,<sup>42</sup> P. Koppenburg,<sup>7</sup> S. Korpar,<sup>12,19</sup> P. Krokovny,<sup>1</sup> Y.-J. Kwon,<sup>48</sup> G. Leder,<sup>10</sup> Y.-J. Lee,<sup>25</sup> T. Lesiak,<sup>26</sup> J. Li,<sup>34</sup> S.-W. Lin,<sup>25</sup> J. MacNaughton,<sup>10</sup> F. Mandl,<sup>10</sup> D. Marlow,<sup>49</sup> T. Matsumoto,<sup>44</sup> A. Matyja,<sup>26</sup> W. Mitaroff,<sup>10</sup> H. Miyake,<sup>30</sup> H. Miyata,<sup>28</sup> T. Mori,<sup>43</sup> T. Nagamine,<sup>41</sup> Y. Nagasaka,<sup>8</sup> E. Nakano,<sup>29</sup> M. Nakao,<sup>7</sup> H. Nakazawa,<sup>7</sup> Z. Natkaniec,<sup>26</sup> S. Nishida,<sup>7</sup> O. Nitoh,<sup>45</sup> S. Ogawa,<sup>39</sup> T. Ohshima,<sup>21</sup> T. Okabe,<sup>21</sup> S. Okuno,<sup>13</sup> S. L. Olsen,<sup>6</sup> W. Ostrowicz,<sup>26</sup> H. Ozaki,<sup>7</sup> H. Palka,<sup>26</sup> C. W. Park,<sup>14</sup> H. Park,<sup>16</sup> N. Parslow,<sup>37</sup> L. E. Piilonen,<sup>47</sup> M. Rozanska,<sup>26</sup> H. Sagawa,<sup>7</sup> Y. Sakai,<sup>7</sup> N. Sato,<sup>21</sup> O. Schneider,<sup>17</sup> J. Schümann,<sup>25</sup> A. J. Schwartz,<sup>4</sup> S. Semenov,<sup>11</sup> M. E. Sevier,<sup>20</sup> H. Shibuya,<sup>39</sup> B. Shwartz,<sup>1</sup> V. Sidorov,<sup>1</sup> A. Somov,<sup>4</sup> N. Soni,<sup>31</sup> R. Stamen,<sup>7</sup> S. Stanič,<sup>46,†</sup> M. Starič,<sup>12</sup> K. Sumisawa,<sup>30</sup> T. Sumiyoshi,<sup>44</sup> S. Suzuki,<sup>33</sup> O. Tajima,<sup>41</sup> F. Takasaki,<sup>7</sup> K. Tamai,<sup>7</sup> N. Tamura,<sup>28</sup> M. Tanaka,<sup>7</sup> G. N. Taylor,<sup>20</sup> Y. Teramoto,<sup>29</sup> K. Trabelsi,<sup>6</sup> T. Tsuboyama,<sup>7</sup> T. Tsukamoto,<sup>7</sup> S. Uehara,<sup>7</sup> T. Uglov,<sup>11</sup> K. Ueno,<sup>25</sup> Y. Unno,<sup>2</sup> S. Uno,<sup>7</sup> G. Varner,<sup>6</sup> K. E. Varvell,<sup>37</sup> C. C. Wang,<sup>25</sup> C. H. Wang,<sup>24</sup> M. Watanabe,<sup>28</sup> B. D. Yabsley,<sup>47</sup> Y. Yamada,<sup>7</sup> A. Yamaguchi,<sup>41</sup> Y. Yamashita,<sup>27</sup> M. Yamauchi,<sup>7</sup> Heyoung Yang,<sup>35</sup> J. Ying,<sup>32</sup> S. L. Zang,<sup>9</sup> J. Zhang,<sup>7</sup> Z. P. Zhang,<sup>34</sup> and D. Žontar<sup>12,18</sup>

(Belle Collaboration)

<sup>1</sup>*Budker Institute of Nuclear Physics, Novosibirsk*<sup>2</sup>*Chiba University, Chiba*<sup>3</sup>*Chonnam National University, Kwangju*<sup>4</sup>*University of Cincinnati, Cincinnati, Ohio 45221, USA*<sup>5</sup>*Gyeongsang National University, Chinju*<sup>6</sup>*University of Hawaii, Honolulu, Hawaii 96822, USA*<sup>7</sup>*High Energy Accelerator Research Organization (KEK), Tsukuba*<sup>8</sup>*Hiroshima Institute of Technology, Hiroshima*<sup>9</sup>*Institute of High Energy Physics, Chinese Academy of Sciences, Beijing*<sup>10</sup>*Institute of High Energy Physics, Vienna*<sup>11</sup>*Institute for Theoretical and Experimental Physics, Moscow*<sup>12</sup>*J. Stefan Institute, Ljubljana*<sup>13</sup>*Kanagawa University, Yokohama*<sup>14</sup>*Korea University, Seoul*<sup>15</sup>*Kyoto University, Kyoto*<sup>16</sup>*Kyungpook National University, Taegu*<sup>17</sup>*Swiss Federal Institute of Technology of Lausanne, EPFL, Lausanne*<sup>18</sup>*University of Ljubljana, Ljubljana*<sup>19</sup>*University of Maribor, Maribor*<sup>20</sup>*University of Melbourne, Victoria*<sup>21</sup>*Nagoya University, Nagoya*<sup>22</sup>*Nara Women's University, Nara*<sup>23</sup>*National Kaohsiung Normal University, Kaohsiung*<sup>24</sup>*National United University, Miao Li*<sup>25</sup>*Department of Physics, National Taiwan University, Taipei*<sup>26</sup>*H. Niewodniczanski Institute of Nuclear Physics, Krakow*<sup>27</sup>*Nihon Dental College, Niigata*<sup>28</sup>*Niigata University, Niigata*<sup>29</sup>*Osaka City University, Osaka*<sup>30</sup>*Osaka University, Osaka*<sup>31</sup>*Panjab University, Chandigarh*<sup>32</sup>*Peking University, Beijing*

<sup>33</sup>Saga University, Saga<sup>34</sup>University of Science and Technology of China, Hefei<sup>35</sup>Seoul National University, Seoul<sup>36</sup>Sungkyunkwan University, Suwon<sup>37</sup>University of Sydney, Sydney NSW<sup>38</sup>Tata Institute of Fundamental Research, Bombay<sup>39</sup>Toho University, Funabashi<sup>40</sup>Tohoku Gakuin University, Tagajo<sup>41</sup>Tohoku University, Sendai<sup>42</sup>Department of Physics, University of Tokyo, Tokyo<sup>43</sup>Tokyo Institute of Technology, Tokyo<sup>44</sup>Tokyo Metropolitan University, Tokyo<sup>45</sup>Tokyo University of Agriculture and Technology, Tokyo<sup>46</sup>University of Tsukuba, Tsukuba<sup>47</sup>Virginia Polytechnic Institute and State University, Blacksburg, Virginia 24061, USA<sup>48</sup>Yonsei University, Seoul<sup>49</sup>Princeton University, Princeton, New Jersey 08545, USA

(Received 14 July 2004; published 15 February 2005)

We report improved measurements of the partial rate asymmetry ( $\mathcal{A}_{CP}$ ) in  $B \rightarrow hh$  decays with  $140 \text{ fb}^{-1}$  of data collected with the Belle detector at the KEKB  $e^+e^-$  collider. Here  $h$  stands for a charged or neutral pion or kaon and in total five decay modes are included:  $K^\mp \pi^\pm$ ,  $K_S^0 \pi^\mp$ ,  $K^\mp \pi^0$ ,  $\pi^\mp \pi^0$ , and  $K_S^0 \pi^0$ . The flavor of the last decay mode is determined from the accompanying  $B$  meson. Using a data sample 4.7 times larger than that of our previous measurement, we find  $\mathcal{A}_{CP}(K^\mp \pi^\pm) = 0.088 \pm 0.035 \pm 0.013$ ,  $2.4\sigma$  from zero. Results for other decay modes are also presented.

DOI: 10.1103/PhysRevD.71.031502

PACS numbers: 13.25.Hw, 11.30.Er, 12.15.Hh, 14.40.Nd

In the standard model (SM)  $CP$  violation arises via the interference of at least two diagrams with comparable amplitudes but different  $CP$  conserving and violating phases. Two-body charmless hadronic  $B$  decays may thus be used to access  $CP$  violation because of the possibility of large interference between tree and penguin diagrams. The angle  $\phi_1$  of the unitarity triangle has been measured with good accuracy using  $b \rightarrow c\bar{c}s$  transitions [1,2]. The focus of the  $B$  factory experiments has now shifted to measurement of the other two angles,  $\phi_2$  and  $\phi_3$ , and to the search for direct  $CP$  violation.

Recent theoretical work suggests that  $\phi_2$  and  $\phi_3$  could be constrained from measurements of branching fractions and partial rate asymmetries in  $B \rightarrow hh$  decays. However, different theoretical approaches such as perturbative QCD (PQCD) [3] and QCD factorization (QCDF) [4–6] lead to different predictions for the partial rate  $CP$  asymmetry, defined as

$$\mathcal{A}_{CP} = \frac{N(\bar{B} \rightarrow \bar{f}) - N(B \rightarrow f)}{N(\bar{B} \rightarrow \bar{f}) + N(B \rightarrow f)}, \quad (1)$$

where  $N(\bar{B} \rightarrow \bar{f})$  is the yield for the  $\bar{B} \rightarrow hh$  decay and  $N(B \rightarrow f)$  denotes that of the charge-conjugate mode. For instance, QCDF predicts a positive asymmetry of less than 10% in  $B \rightarrow K\pi$  while PQCD favors a negative value ranging from  $-10\%$  to  $-30\%$ . Although there are large

uncertainties related to hadronic effects, more precise measurements of partial rate asymmetries would discriminate between the theoretical approaches. Furthermore, if a sizable asymmetry is observed for a mode where only one diagram contributes in the SM, this may be an indication of new physics.

In the search reported in this paper, five decay modes are considered:  $K^\mp \pi^\pm$ ,  $K_S^0 \pi^\mp$ ,  $K^\mp \pi^0$ ,  $\pi^\mp \pi^0$ , and  $K_S^0 \pi^0$ . (In the following, charge-conjugate modes are implied unless otherwise stated.) The data sample used in this study corresponds to  $140 \text{ fb}^{-1}$  ( $152 \times 10^6 BB$  pairs), which is 1.8 times larger than that used in the previous study for the  $K_S^0 \pi^-$  mode [7], and is 4.7 times larger than that used for the other modes [8]. The observation of large  $CP$  violation in  $B^0 \rightarrow \pi^+ \pi^-$  at Belle has been recently reported elsewhere [9].

The data were collected with the Belle detector at the KEKB  $e^+e^-$  collider. KEKB is an asymmetric collider (3.5 on 8 GeV) that operates at the  $Y(4S)$  resonance ( $\sqrt{s} = 10.58 \text{ GeV}$ ). The Belle detector is a large-solid-angle magnetic spectrometer consisting of a three-layer silicon vertex detector, a 50-layer central drift chamber (CDC), a system of aerogel threshold Cherenkov counters (ACC), time-of-flight scintillation counters (TOF), and an array of CsI crystals (ECL) located inside a superconducting solenoid that provides 1.5 T magnetic field. An iron flux return located outside is instrumented as a  $K_L^0$  and muon identifier. A detailed description of the Belle detector can be found in Ref. [10].

The  $B$  candidate selection is the same as described in Ref. [11]. Charged tracks are required to originate from the

\*On leave from Fermi National Accelerator Laboratory, Batavia, IL 60510.

†On leave from Nova Gorica Polytechnic, Nova Gorica.

interaction point (IP). Charged kaons and pions are identified using  $dE/dx$  information and Cherenkov light yields in the ACC. The  $dE/dx$  and ACC information are combined to form a  $K-\pi$  likelihood ratio,  $\mathcal{R}(K\pi) = \mathcal{L}_K/(\mathcal{L}_K + \mathcal{L}_\pi)$ , where  $\mathcal{L}_{K/\pi}$  is the likelihood of kaon/pion. Charged tracks with  $\mathcal{R}(K\pi) > 0.6$  are regarded as kaons and  $\mathcal{R}(K\pi) < 0.4$  as pions. The  $K/\pi$  identification efficiencies and misidentification rates are determined from a sample of kinematically identified  $D^{*+} \rightarrow D^0\pi^+$ ,  $D^0 \rightarrow K^-\pi^+$  decays. For positively charged tracks, the identification efficiencies and fake rates for  $K(\pi)$  are  $83.7 \pm 0.2\%$  ( $91.3 \pm 0.2\%$ ) and  $10.7 \pm 0.2\%$  ( $5.1 \pm 0.1\%$ ) and for negatively charged tracks, they are  $84.7 \pm 0.2\%$  ( $90.5 \pm 0.2\%$ ) and  $10.0 \pm 0.2\%$  ( $5.7 \pm 0.1\%$ ), respectively. Furthermore, charged tracks that are positively identified as electrons are rejected.

Candidate  $\pi^0$  mesons are reconstructed by combining two photons with invariant mass between 115 MeV/ $c^2$  and 152 MeV/ $c^2$ , which corresponds to  $\pm 2.5$  standard deviations. Each photon is required to have a minimum energy of 50 MeV in the barrel region ( $32^\circ < \theta_\gamma < 129^\circ$ ) or 100 MeV in the end-cap region ( $17^\circ < \theta_\gamma < 32^\circ$  or  $129^\circ < \theta_\gamma < 150^\circ$ ), where  $\theta_\gamma$  denotes the polar angle of the photon with respect to the beam line. To further reduce the combinatorial background,  $\pi^0$  candidates with small decay angles ( $\cos\theta^* > 0.95$ ) are rejected, where  $\theta^*$  is the angle between a  $\pi^0$  boost direction from the laboratory frame and its  $\gamma$  daughters in the  $\pi^0$  rest frame. Candidate  $K_S^0$  mesons are reconstructed from pairs of oppositely charged tracks with invariant mass in the range  $480 \text{ MeV}/c^2 < M_{\pi\pi} < 516 \text{ MeV}/c^2$ . Each candidate must have a displaced vertex and a flight direction consistent with a  $K_S^0$  originating from the IP.

Two variables are used to identify  $B$  candidates: the beam-constrained mass,  $M_{bc} = \sqrt{E_{\text{beam}}^{*2} - p_B^{*2}}$ , and the energy difference,  $\Delta E = E_B^* - E_{\text{beam}}^*$ , where  $E_{\text{beam}}^*$  is the beam energy and  $E_B^*$  and  $p_B^*$  are the reconstructed energy and momentum of the  $B$  candidates in the center-of-mass (CM) frame. Events with  $M_{bc} > 5.20 \text{ GeV}/c^2$  and  $-0.3 \text{ GeV} < \Delta E < 0.3 \text{ GeV}$  are selected for the final analysis for modes with  $\pi^0$ 's in the final state and  $-0.3 \text{ GeV} < \Delta E < 0.5 \text{ GeV}$  for the modes without. For the  $K_S^0\pi^0$  mode, events with  $\Delta E < -0.1 \text{ GeV}$  are excluded to remove the background from charmless  $B$  decays.

The dominant background is from  $e^+e^- \rightarrow q\bar{q}$  ( $q = u, d, s, c$ ) continuum events. To distinguish the signal from the jetlike continuum background, event topology variables and  $B$  flavor tagging information are employed. We combine a set of modified Fox-Wolfram moments [12] into a Fisher discriminant. The probability density functions (PDF) for this discriminant, and the cosine of the angle between the  $B$  flight direction and the  $z$  axis, are obtained using signal and continuum Monte Carlo (MC)

events. These two variables are then combined to form a likelihood ratio  $\mathcal{R} = \mathcal{L}_s/(\mathcal{L}_s + \mathcal{L}_{q\bar{q}})$ , where  $\mathcal{L}_{s(q\bar{q})}$  is the product of signal ( $q\bar{q}$ ) probability densities. Additional background discrimination is provided by  $B$  flavor tagging. The Belle standard flavor tagging algorithm [13] gives two outputs: a discrete variable indicating the flavor of the tagging  $B$  and the MC-determined dilution factor  $r$ , which ranges from zero for no flavor information to unity for unambiguous flavor assignment. An event that contains a lepton ( $r$  close to unity) is more likely to be a  $B\bar{B}$  event so a looser  $\mathcal{R}$  requirement can be applied. We combine  $\mathcal{R}$  and  $r$  to form a multidimensional likelihood ratio (MDLR), defined as  $\mathcal{L}_s^{\text{MDLR}}/(\mathcal{L}_s^{\text{MDLR}} + \mathcal{L}_{q\bar{q}}^{\text{MDLR}})$ , where  $\mathcal{L}_{s(q\bar{q})}^{\text{MDLR}}$  denotes the likelihood of the signal ( $q\bar{q}$ ) in the  $\mathcal{R}-r$  space. The continuum background is reduced by applying a selection requirement on the MDLR. The requirement for each mode is optimized according to the figure of merit defined as  $N_s^{\text{exp}}/\sqrt{N_s^{\text{exp}} + N_{q\bar{q}}^{\text{exp}}}$ , where  $N_s^{\text{exp}}$  denotes the expected signal yields based on our previous branching fraction measurements [11] and  $N_{q\bar{q}}^{\text{exp}}$  denotes the expected  $q\bar{q}$  yields from sideband data ( $M_{bc} < 5.26 \text{ GeV}/c^2$ ). A typical requirement suppresses 94%–98% of the continuum background while retaining 50%–65% of the signal.

Backgrounds from  $Y(4S) \rightarrow B\bar{B}$  events are investigated using a large MC sample. After the MDLR requirement, we find a small charmless three-body background at low  $\Delta E$ , and reflections from other  $B \rightarrow hh$  decays due to  $K-\pi$  misidentification.

The signal yields are extracted by applying unbinned two-dimensional maximum likelihood (ML) fits to the ( $M_{bc}$  and  $\Delta E$ ) distributions of the  $B$  and  $\bar{B}$  samples. The likelihood for each mode is defined as

$$\mathcal{L} = \frac{e^{-\sum_j N_j}}{N!} \times \prod_i \left( \sum_j N_j \mathcal{P}_j \right), \quad (2)$$

$$\mathcal{P}_j = \frac{1}{2} [1 - q_i \cdot \mathcal{A}_{CPj}] P_j(M_{bc}, \Delta E), \quad (3)$$

where  $N$  is the total number of events;  $i$  is the identifier of the  $i$ th event;  $N_j$  is the number of events for the category  $j$ , which corresponds to either signal,  $q\bar{q}$  continuum, a reflection due to  $K-\pi$  misidentification, or background from other charmless three-body  $B$  decays;  $P(M_{bc}, \Delta E)$  is the two-dimensional PDF of  $M_{bc}$  and  $\Delta E$ ; and  $q$  indicates the  $B$  meson flavor,  $B(q = +1)$  or  $\bar{B}(q = -1)$ .

Unlike the other four  $hh$  decay modes, the flavor of the  $B$  meson in the  $K_S^0\pi^0$  channel is not self-tagged and must be determined from the accompanying  $B$  meson. To account for the effect of  $B\bar{B}$  mixing and imperfect tagging, the term  $\mathcal{A}_{CP}$  for the signal in Eq. (3) has to be replaced by  $\mathcal{A}_{CP}(1 - 2\chi_d)(1 - 2w_l)$ , where  $\chi_d = 0.181 \pm 0.004$  [14] is the time-integrated mixing parameter and  $w_l$  is the wrong-tag fraction. The  $K_S^0\pi^0$  sample is divided into

TABLE I. The fitted signal yields and  $\mathcal{A}_{CP}$  results for individual modes.

Mode	Signal yield	$\mathcal{A}_{CP}$
$K^{\mp}\pi^{\pm}$	$1029.8 \pm 35.3$	$-0.088 \pm 0.035 \pm 0.013$
$K_S^0\pi^{\mp}$	$429.8 \pm 23.0$	$+0.05 \pm 0.05 \pm 0.01$
$K^{\mp}\pi^0$	$516.5 \pm 29.4$	$+0.06 \pm 0.06 \pm 0.02$
$\pi^{\mp}\pi^0$	$235.6 \pm 23.4$	$-0.00 \pm 0.10 \pm 0.02$
$K_S^0\pi^0$	$96.6 \pm 11.8$	$+0.16 \pm 0.29 \pm 0.05$

six  $r$  bins, and the  $r$ -dependent wrong-tag fractions,  $w_l$  ( $l = 1, \dots, 6$ ), are determined using a high statistics sample of self-tagged  $B^0 \rightarrow D^{(*)-}\pi^+$ ,  $D^{*-}\rho^+$  and  $D^{*-}\ell^+\nu$  events and their charge conjugates [15]. No  $K-\pi$  misidentification reflection or other backgrounds from charmless three-body  $B$  decays are included in this mode.

The yields and asymmetries for the signal and backgrounds are allowed to float in all modes except for  $K_S^0\pi^0$ , in which the background asymmetry is set to zero. Since the  $K^+\pi^0$  and  $\pi^+\pi^0$  reflections are difficult to distinguish with  $\Delta E$  and  $M_{bc}$ , we fit these two modes simultaneously with a fixed reflection-to-signal ratio based on the  $K-\pi$  identification efficiencies and fake rates. All the signal PDFs [ $P(M_{bc}, \Delta E)$ ] are obtained using MC simulation. No strong correlations between  $M_{bc}$  and  $\Delta E$  are found

for the  $K_S^0\pi^-$  and  $K^-\pi^+$  signals. Therefore, their PDFs are modeled by products of single Gaussians for  $M_{bc}$  and double Gaussians for  $\Delta E$ . For the modes with  $\pi^0$ 's in the final state, there are correlations between  $M_{bc}$  and  $\Delta E$  in the tails of the signals; hence, their PDFs are described by smoothed two-dimensional histograms. Discrepancies between the signal peak positions in data and MC are calibrated using  $B^+ \rightarrow \bar{D}^0\pi^+$  decays, where the  $\bar{D}^0 \rightarrow K^+\pi^-\pi^0$  subdecay is used for the modes with a  $\pi^0$  meson while  $\bar{D}^0 \rightarrow K^+\pi^-$  is used for the other modes. The MC-predicted  $\Delta E$  resolutions are verified using the invariant mass distributions of high momentum  $D$  mesons. The decay mode  $\bar{D}^0 \rightarrow K^+\pi^-$  is used for  $B^0 \rightarrow K^+\pi^-$ ,  $D^+ \rightarrow K_S^0\pi^+$  for  $B^+ \rightarrow K_S^0\pi^+$ , and  $\bar{D}^0 \rightarrow K^+\pi^-\pi^0$  for the modes with a  $\pi^0$  in the final state. The parameters that describe the shape of the PDFs are fixed in all of the fits.

The background PDFs for continuum events are modeled by an ARGUS function [16] for the  $M_{bc}$  distribution and a 1st or 2nd order polynomial for the  $\Delta E$  distribution, assuming no correlations between the two. A large MC sample is used to investigate the background from charmless  $B$  decays and a smoothed two-dimensional histogram is taken as the PDF.

Table I gives the signal yields and  $\mathcal{A}_{CP}$  values for each mode. The asymmetries for the background components are consistent with zero. The errors on  $\mathcal{A}_{CP}$  are deter-

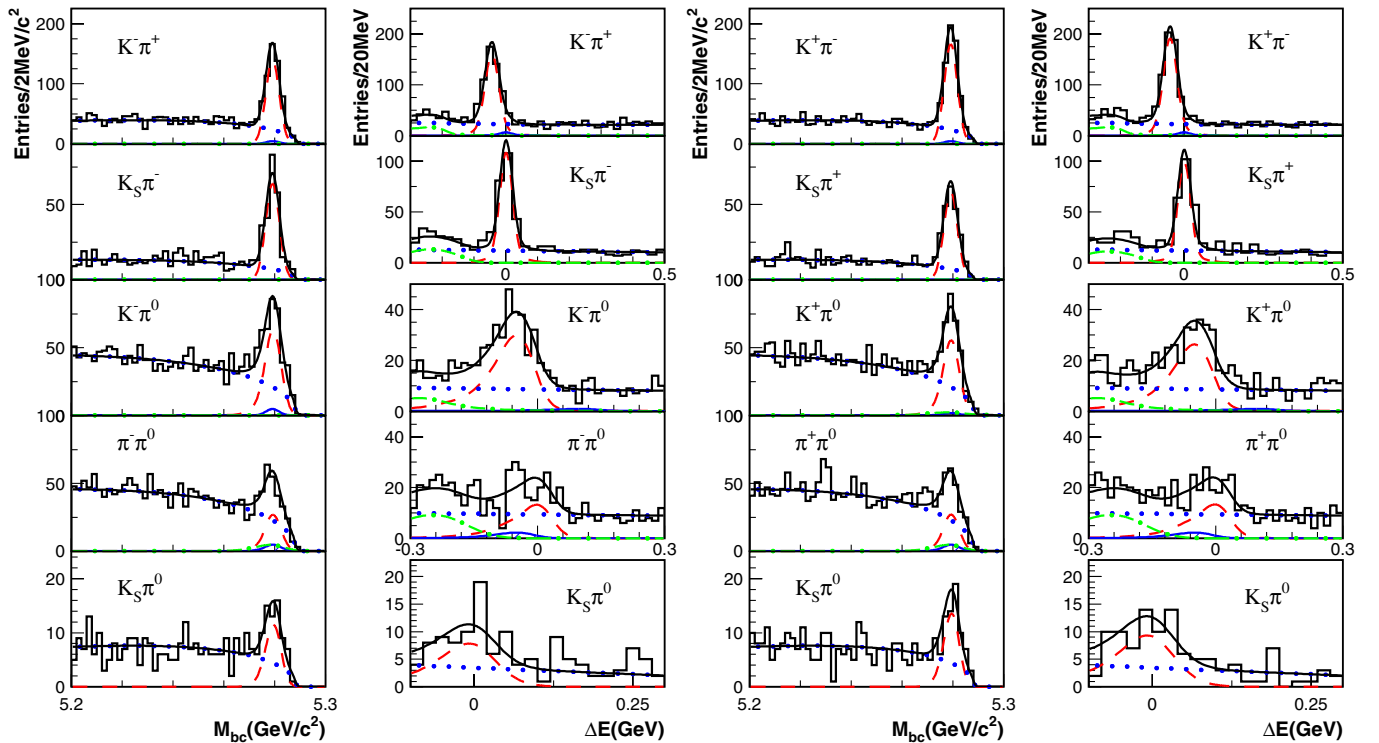


FIG. 1 (color online).  $M_{bc}$  (left) and  $\Delta E$  (right) distributions for  $\bar{B}$  (left two columns) and  $B$  (right two columns) candidates reconstructed in the  $K^{\mp}\pi^{\pm}$ ,  $K_S^0\pi^{\mp}$ ,  $K^{\mp}\pi^0$ ,  $\pi^{\mp}\pi^0$ , and  $K_S^0\pi^0$  modes (from top to bottom). The histograms represent the data, while the curves represent the various components from the fit: signal (dashed line), continuum (dotted line), three-body  $B$  decays (dash-dotted line), background from misidentification (hatched line), and sum of all components (solid line).

mined from the ML fit and are consistent with MC expectations. Projections of the fits are shown in Fig. 1. The systematic errors from fitting are estimated by checking the deviations of the  $\mathcal{A}_{CP}$  after varying each parameter of the signal PDFs by 1 standard deviation. The uncertainty in modeling the three-body background is studied by excluding the low  $\Delta E$  region ( $< -0.12$  GeV) and repeating the fit. For the  $K^+\pi^0$  and  $\pi^+\pi^0$  modes, the uncertainty on the reflection-to-signal ratios obtained from  $D^*$  control samples are included in the systematic error, with contributions of  $\pm 0.006$  and  $\pm 0.009$  for the  $K^+\pi^0$  and  $\pi^+\pi^0$  modes, respectively. The uncertainties in the mixing parameter  $\chi_d$  and wrong-tag fraction  $w_r$  are included in the systematic error for the  $K_S^0\pi^0$  mode. At each step, the deviation in  $\mathcal{A}_{CP}$  is added in quadrature to provide the systematic errors due to fitting, which are  $+0.014 - 0.020$  for the  $K_S^0\pi^0$  mode and less than 0.01 for all other modes. A possible detector bias in  $\mathcal{A}_{CP}$  is investigated using the  $B^+ \rightarrow \bar{D}^0\pi^+$  samples, assuming null charge asymmetries in the production. In this control sample, the same continuum suppression and fitting procedures are applied. To mimic the  $B^0 \rightarrow K_S^0\pi^0$  analysis, the flavor of the  $B$  meson is determined using flavor tagging information from the associated  $B$ . Results of these null asymmetry checks are shown in Table II. The final systematic errors are then obtained by quadratically summing the errors from the null asymmetry tests and the fitting systematics.

In this study, the partial rate asymmetry  $\mathcal{A}_{CP}(K^-\pi^+)$  is found to be  $-0.088 \pm 0.035 \pm 0.013$ , which is  $2.4\sigma$  from zero. The corresponding 90% confidence level (C.L.) interval is  $-0.15 < \mathcal{A}_{CP}(K^-\pi^+) < -0.03$ . Our central

TABLE II. Results of null asymmetry cross-checks.

Mode	$B \rightarrow D(\rightarrow K\pi)\pi$	$B \rightarrow D(\rightarrow K\pi\pi^0)\pi$	$B \rightarrow D\pi$ tagged
$N_{\text{sig}}$	$6290.2 \pm 79.8$	$7982.1 \pm 101.8$	$8726.1 \pm 86.4$
$\mathcal{A}_{CP}$	$0.002 \pm 0.013$	$0.012 \pm 0.012$	$-0.027 \pm 0.029$

value is similar to that reported by *BABAR*,  $\mathcal{A}_{CP}(K^-\pi^+) = -0.107 \pm 0.041 \pm 0.013$  [17], indicating that the partial rate asymmetry may be negative [18]. Theoretical predictions from different approaches suggest that  $\mathcal{A}_{CP}(K^-\pi^+)$  and  $\mathcal{A}_{CP}(K^+\pi^0)$  should have the same sign. The uncertainty in our result for  $\mathcal{A}_{CP}(K^+\pi^0)$  is large enough for it to be consistent with this expectation. We set a 90% C.L. interval of  $-0.04 < \mathcal{A}_{CP}(K^+\pi^0) < 0.16$ . Since no evidence of direct  $CP$  violation is observed in the decays  $B^- \rightarrow K_S^0\pi^-$  and  $B^+ \rightarrow \pi^+\pi^0$ , we set 90% C.L. intervals:  $-0.04 < \mathcal{A}_{CP}(K_S^0\pi^-) < 0.13$ ,  $-0.17 < \mathcal{A}_{CP}(\pi^+\pi^0) < 0.16$ , and  $-0.33 < \mathcal{A}_{CP}(K_S^0\pi^0) < 0.64$ .

We thank the KEKB group for the excellent operation of the accelerator, the KEK Cryogenics group for the efficient operation of the solenoid, and the KEK computer group and the NII for valuable computing and Super-SINET network support. We acknowledge support from MEXT and JSPS (Japan); ARC and DEST (Australia); NSFC (Contract No. 10175071, China); DST (India); the BK21 program of MOEHRD and the CHEP SRC program of KOSEF (Korea); KBN (Contract No. 2P03B 01324, Poland); MIST (Russia); MESS (Slovenia); NSC and MOE (Taiwan); and DOE (USA).

- [1] Belle Collaboration, K. Abe *et al.*, Phys. Rev. D **66**, 071102(R) (2002).
- [2] *BABAR* Collaboration, B. Aubert *et al.*, Phys. Rev. Lett. **89**, 201802 (2002).
- [3] Y.-Y. Keum and A.I. Sanda, Phys. Rev. D **67**, 054009 (2003).
- [4] M. Gronau and J.L. Rosner, Phys. Lett. B **572**, 43 (2003).
- [5] M. Gronau and J.L. Rosner, Phys. Rev. D **65**, 013004 (2002).
- [6] M. Beneke *et al.*, Nucl. Phys. **B606**, 245 (2001).
- [7] Belle Collaboration, Y. Unno *et al.*, Phys. Rev. D **68**, 011103 (2003).
- [8] Belle Collaboration, B. C. K. Casey *et al.*, Phys. Rev. D **66**, 092002 (2002).
- [9] Belle Collaboration, K. Abe *et al.*, Phys. Rev. Lett. **93**, 021601 (2004).
- [10] Belle Collaboration, A. Abashian *et al.*, Nucl. Instrum. Methods Phys. Res., Sect. A **479**, 117 (2002).
- [11] Belle Collaboration, Y. Chao *et al.*, Phys. Rev. D **69**, 111102(R) (2004).
- [12] The Fox-Wolfram moments were introduced in G. C. Fox and S. Wolfram, Phys. Rev. Lett. **41**, 1581 (1978); The modified moments used in this paper are described in Belle Collaboration, S.H. Lee *et al.*, Phys. Rev. Lett. **91**, 261801 (2003).
- [13] H. Kakuno *et al.*, Nucl. Instrum. Methods Phys. Res., Sect. A **533**, 516 (2004).
- [14] Particle Data Group, K. Hagiwara *et al.*, Phys. Rev. D **66**, 010001 (2002).
- [15] Belle Collaboration, K. Abe *et al.*, hep-ex/0308036.
- [16] ARGUS Collaboration, H. Albrecht *et al.*, Phys. Lett. B **241**, 278 (1990).
- [17] *BABAR* Collaboration, M. Bona, hep-ex/0404038.
- [18] After this paper was submitted to PRD RC, measurements with larger datasets were reported by *BABAR* [19] and Belle [20] that together establish the presence of direct  $CP$  violation in the  $B$  meson system.
- [19] *BABAR* Collaboration, B. Aubert *et al.*, Phys. Rev. Lett. **93**, 131801 (2004).
- [20] Belle Collaboration, Y. Chao *et al.*, Phys. Rev. Lett. **93**, 191802 (2004).